X-695-77-206

MARINER 10
MAGNETIC FIELD OBSERVATIONS OF THE VENUS WAKE

R P. LEPPING
K. W. BEHANNON

AUGUST 1977

GSFC — GODDARD SPACE FLIGHT CENTER —
GREENBELT, MARYLAND

X-695-77-206

MARINER 10 MAGNETIC FIELD OBSERVATIONS OF THE VENUS WAKE

by

R. P. Lepping
K. W. Behannon

Laboratory for Extraterrestrial Physics
NASA/Goddard Space Flight Center
Greenbelt, Maryland 20771

August 1977

ABSTRACT

Magnetic field measurements made over a 21-hour interval during the Mariner 10 encounter with Venus were used to study the down-stream region of the solar wind-Venus interaction over a distance of $\approx 100\ R_V$. Mariner 10 encountered Venus on 5 February 1974 with closest approach at 1702 U.T. For most of the day before closest approach the spacecraft was located in a sheath-like region which was apparently bounded by the planet's bow shock on the outer side and either a planetary "wake boundary" or transient boundary-like feature on the inner side. The spacecraft made multiple encounters with the wake-like boundary during the 21-hour interval with an increasing frequency as it approached the planet. Each pass into the wake boundary from the sheath region was consistently characterized by a slight decrease in magnetic field magnitude, a marked increase in the frequency and amplitude of field fluctuations, and a systematic clockwise rotation of the field direction when viewed from above the plane of Venus' orbit. These boundary crossings were not accompanied strictly by hydromagnetic directional discontinuities, however, but occasionally ($\sim$ 1/3 of crossings) such a discontinuity was sufficiently close to the crossing zone to be considered part of the boundary transition. There was a significantly larger number of discontinuities in the overall 21-hour period than was observed on average during other comparable periods both before and after encounter. A simple large-scale draped-field model in the sense of a magnetic "comet tail" was found not to hold for the downstream region. The sporadic observation of the wake during the near encounter period may have been controlled by changes in the direction of the interplanetary field.

1. INTRODUCTION

This paper reports on the analysis of magnetic field observations by the Mariner 10 spacecraft during approximately a one day period ending a few hours beyond Venus encounter on 5 February 1974. Since this dual planet mission was optimized for investigations of Mercury, the spacecraft trajectory at Venus was constrained in such a way that it allowed a limited study of the region downstream from Venus. For this purpose the trajectory had a distinct advantage over those of previous (and known future) missions to the planet in that for several days preceding encounter the spacecraft followed a trajectory which, except for the final hour before closest approach, remained approximately on the surface of a cone of half-angle 9.5^{o} with axis along the planet-sun line. This angle was only slightly smaller than the estimated asymptotic planetary bow shock angle ($\approx 11^{o}$).

Unfortunately, Mariner 10 could not penetrate very deeply into a downstream wake (or magnetic tail) region, since it remained outside the geometrical shadow region throughout the entire approach to the planet. This is most disadvantageous close to Venus, where interaction effects would be expected to be strongest but where the possibility of sampling the interior of a wake via the "flapping" of the wake in the solar wind is smallest. This lack of possible deep-wake observations complicates the interpretation of pre and near encounter measurements. However, the observations suggest that over a fortuitiously long distance the spacecraft crossed repeatedly for brief periods from a sheath-like region occurring interior to the estimated position of the bow shock, which was never observed in the

downstream data, into what appeared to be a wake of Venus enclosed by the sheath. We use the term "wake" here to include either a true stationary feature or possibly a transient region approximately bounded by a conical surface.

Overviews of the present state of knowledge and speculations on the magnetic field and particle environment of Venus are given by Bauer et al. (1977) and Yeates et al. (1977). We give here some additional introductory comments. As Siscoe (1977) recently pointed out, Venus' position in the hierarchy of planetary magnetospheres is now uncertain in light of the broad range of estimates of an upper bound for a possible magnetic moment for the planet. If the lowest estimate of 2×10^{22} gauss-cm^3 by Dolginov et al. (1976) is correct, Venus represents possibly the only example of a pure solar wind-planetary atmosphere interaction in the solar system. If the highest moment estimate (6.5×10^{22} gauss-cm^3 by Russell, 1976a, or $< 8 \times 10^{22}$ gauss-cm^3 by Bridge et al. 1967; also see Ness (1976)) is correct, the situation represents "the extreme limit of a continuum of magnetic interactions in which the field becomes so weak that the force of the solar wind is opposed mainly by contact with the physical material of the planet, in this instance the planet's ionosphere. In either case, the atmosphere exerts an overwhelming control over plasma and field structures" (Siscoe, 1977).

The Mariner 10 magnetic field measurements (Ness et al., 1974) have confirmed observations from previous missions (Bridge et al., 1967 and Dolginov et al., 1968, 1969) that the solar wind-Venus interaction produces a planetary bow shock. Russell (1977a,b) has suggested

that due to possible significant solar wind absorption by the Venusian atmosphere during the Mariner 10 encounter, the bow shock at that time probably intersected the ionopause at the stagnation point, although earlier observations suggest that it usually is detached (Bridge et al., 1967; Dolginov et al., 1968, 1969; Rizzi, 1971). Ness (1977) has argued that Russell's interpretation of this issue is questionable because of possible inadequate bow shock modeling and incorrect error analysis.

The primary purposes of this paper are: (1) to generally characterize the various magnetic field regions encountered behind and near the planet, (2) to present an argument that the magnetic field signatures observed were consistent with observation of a wake, or at least the boundary region of a wake, interior to a sheath-like region, (3) to examine in detail the fluctuation and discontinuity features of these regions and compare them to those of the interplanetary medium and, finally (4) to summarize how these new features contribute to our understanding of the solar wind-Venus interaction.

2. INSTRUMENTATION AND TRAJECTORY

The Mariner 10 instrument configuration represented the first use of the dual three-axis magnetometer technique described by Ness et al. (1971). This configuration was used successfully to remove the effects of a large and variable spacecraft field from the measurements (Ness et al. 1974). The calibration techniques and further formulation of the dual magnetometer method as used on Mariner 10 have been discussed by Lepping et al. (1975).

Both magnetometer sensor sets were three axis fluxgates with a sample rate of 25 samples/sec. Each sensor operated automatically in

one of two sensitivity ranges ($\pm$ 16 and $\pm$ 128γ full scale), quantized to 10 bits/component. This yielded quantization step sizes of 0.030γ and 0.26γ in the low and high ranges, respectively. Individual sensor RMS noise levels ranged between 0.030 and 0.069γ, and the instrument bandwidth was 0 to 12.5 Hz. The spacecraft field variations were slow enough during most of the mission so that 3 sec average spacecraft field estimates allowed accurate estimation of the ambient field every 40 msec. The experiment hardware characteristics have been described in detail by Seek et al. (1977).

Hourly average ambient fields observed during the cruise portions of the primary mission, including the period of approach to Venus, have been presented by Behannon and Ottens (1976). A document which presents plots of the magnetic field in 6-sec average form and associated spacecraft trajectory for 4 and 5 February 1974, including a comprehensive bibliography on Venus, is also available (Lepping et al., 1977).

In Figure 1 we show the Mariner 10 trajectory in the vicinity of Venus in Venus Orbital (VO) coordinates for approximately 70 R_V (Venus radii) before encounter. The VO coordinate system will be used throughout this study for both trajectory and data representation. It is defined in the following way: Z_{VO} is perpendicular to the orbital plane of Venus, positive northward; X_{VO} is along the Venus-sun line, positive sunward; Y_{VO} completes the right-handed system by $\hat{Y}_{VO} = \hat{Z}_{VO} \times \hat{X}_{VO}$ i.e., $+Y_{VO}$ is approximately opposite to the direction of planetary orbital motion; and the system is planet-centered.

In order to estimate a probable location for Venus's bow shock over tens of planetary radii, we determine an asymptotic value for the angle σ_B

between the far shock and the X_{VO} axis using the expression for this angle given by Dryer and Heckman (1967),

$$\sigma_B = \sin^{-1}\left(\frac{1}{M_\infty^*}\right),$$

where

$$M_\infty^* = \sqrt{\frac{M_\infty^2 \; M_{A,\infty}^2}{M_\infty^2 + M_{A,\infty}^2 - 1}},$$

and where M_∞ and $M_{A,\infty}$ are the upstream sonic and Alvenic mach numbers, respectively. Since the direction of the interplanetary magnetic field (IMF) is not known during this time, nor the exact solar wind characteristics, attempting a more exact estimation of the shock location is not realistic (see Spreiter, 1976).

Assuming a field of $\sim 10\gamma$, a solar wind proton number density of $\sim 10\ cm^{-1}$, and a solar wind speed of 420 km/sec based on average post-encounter values (K. Ogilvie, private communication) yields an Alfvén mach number of 6.1. A typical proton solar wind temperature of $9 \times 10^4\ ^oK$ yields accordingly a sonic mach number of 12. The composite mach number is then $M_\infty^* \approx 5.4$ and the asymptotic bow shock angle is therefore $\sim 11^o$.

To complete the bow shock estimate we develop a scaling ratio based on a comparison with earth's bow shock. Since the height of Venus' ionosphere on the sunward side is estimated to be ≈ 450 Km (Ness et al., 1974) and the planetary radius (R_V) is 6050 Km, the ionosphere, assumed to be the obstacle to solar wind flow, is approximately a sphere of radius ≈ 6500 Km. The earth's obstacle size is $\approx 11\ R_E$ or 70,200 Km. Hence, the scaling ratio from Earth to Venus is 10.8. Using the earth's large-scale bow shock

as estimated by Villante (1976) as a guide, the angle $\sigma_B \approx 11^o$, and a shock sub-solar distance above the planet of $\sim 0.5\ R_V$, again scaled from the earth's case, we arrive at the estimated bow shock position shown in Figure 1.

The spacecraft trajectory appears to lie fairly well within the estimated bow shock location for the period of interest, until after closest approach to the planet, where a pulsation bow shock crossing has been identified (Ness et al. 1974, and Bridge, et al. 1974). None of the pre-closest-approach data indicate bow shock crossings either in terms of general magnetic signatures or by satisfying the field and plasma conservation conditions, and, in fact, for all prospective cases examined there were flagrant violations of the conservation conditions in terms of the sign of the difference quantities (K. Ogilive, private communication). Notice that the spacecraft remained close to the X-Z plane (shown in the lower panel) at positive Z (upper panel) throughout. The geometrical (or optical) shadow of the planet is shown for reference.

3. NEAR VENUS REGION

Figure 2 shows 6 sec magnetic field averages and RMS's from $\sim$ 5 1/2 hours before encounter (closest approach at 1702 U.T.) to $\sim$ 2 hours after encounter and gives the near-planet trajectory in cylindrical coordinates (i.e. $\sqrt{Y_{vo}^2 + Z_{vo}^2}$ vs X_{vo}). A preliminary discussion of the near-planet field observations has been given by Ness et al. (1974); we will be concerned here primarily with the region where $X_{vo} \leq 0$. The field had a generally disturbed appearance (variable in direction and magnitude and reduced average magnitude) from 1350 U.T. to the pulsation bow shock

at 1652 $\pm$ 1 U.T. with only a few periods of respite, such as 1543 to 1558 U.T. Earlier the opposite situation was the case; prior to 1350 U.T. the field had a generally quiet appearance with disturbed intervals such as the one from 1245 to 1256 U.T. being the exception.

In Figure 3 (see Figure 4 of Whang et al., 1974), are shown certain characteristics of the field observations for approximately two hours before encounter. These include the variances (in γ^2) for the field computed for 1.2, 6, and 42 sec periods (and averaged over 42 sec each), the magnitude of the field F, and the magnitude-normalized-RMS δ_{42}/F, as well as the angles ω_B (solid curve) and ω_T (dashed line) which are defined in the following way (see Figure 4): ω_B is the angle between $\vec{B}_P$ and $\vec{B}_Z$ where $\vec{B}_P = B_Y \hat{Y} + B_Z \hat{Z}$, i.e.,

$$\omega_B = \tan^{-1} (B_Y/B_Z),$$

and ω_T is the angle that the projection of the spacecraft position-vector into the Y-Z plane makes with the Y-axis. [Notice that the X-dimension is of no direct interest in this view.] Whenever ω_T and ω_B are equal it is easily seen that at the spacecraft position the total field must be locally tangent to a cylinder whose axis is the X_{VO}-axis. One possible interpretation is that these periods of local tangency reflect fields on the inside of a tail-sheath boundary (Whang et al., 1974). However, the measured field during the cylindrical tangency periods (i.e. when $\omega_B \approx \omega_T$) was not predominantly in the X_{VO} direction, so that a typically magnetotail-like configuration was not observed. An alternate view that we believe more likely is that such fields represent the exterior or sheath region. There the field would be

expected to assume approximately a circular configuration in the Y-Z plane as it seeks to avoid the spherical obstacle of Venus' ionosphere and follow the plasma flow in the sheath. Periods during which $\omega_B \approx \omega_T$ were observed at least as early as 1300 U.T., although such apparent cylindrical symmetry so far from Venus could simply have been fortuitous.

Figure 3 shows that the periods when $\omega_B \approx \omega_T$ were also periods of higher field magnitude and lower fluctuation levels. We shall demonstrate in the following sections that at greater distances from the planet these conditions were consistent with being located in the sheath region, and that there was good continuity of these properties into the near-planet region, except for the period beginning just prior to closest approach. The spacecraft had crossed over to the dawn side of the planet at that time. It is possible that from $\sim$ 1548 U.T. onward, until the bow shock began to be observed at $\sim$ 1651 U.T., the spacecraft was exclusively in the sheath, but that the sheath in the near-shock region was of a different character from that previously seen due perhaps to field line connection to the pulsation portion of the shock (Greenstadt et al., 1968, 1970; Greenstadt, 1971).

4. WAKE OBSERVATIONS AND STATISTICAL STUDY

In Figure 1 we identify with black rectangles along the trajectory (top panel) what we define as disturbed regions. These regions are those which, as mentioned in the discussion of Figure 2, are characterized by enhanced fluctuation levels, depressed field magnitudes and rotated directions; these regions will be defined more precisely and discussed below. Between these disturbed regions the field is noticeably quieter according to the same criteria.

In Figure 5 we give examples of typical quiet and disturbed regions. The top panel shows 6 sec averages for a two-hour period of magnitude-longitude-latitude (F, ϕ, θ) representation. In the bottom panel we show an expanded view of 40 msec field component data for a 3 min period which spans a quiet-disturbed boundary. Identification of a region as quiet or disturbed was based on the visual inspection of plots of 6 sec averages, with quiet regions subjectively defined as those with relatively higher magnitude and lower RMS on average and disturbed regions comprising those which on average had distinctly lower magnitude and higher RMS than quiet regions. Here RMS is defined as $\sqrt{RMS_x^2 + RMS_y^2 + RMS_z^2}$, RMS_x being the root mean square deviation of the x-component based on 1.2 sec averages, etc. The general assessment of disturbed region fields as being "disturbed" or "variable" in appearance applies to all of the three field parameters F, ϕ and θ. It must be stressed that these definitions are based on relative terms since they are meant to refer to the relative appearance of adjacent regions across a boundary. For example, a "quiet" region close to the planet may appear more disturbed than a "disturbed" region much further from the planet. Also the quiet regions are quiet relative to their disturbed neighbors but generally more disturbed than the interplanetary field (see Section 6), giving the impression of a sheath-like field. On occasion an angle change occurred at or very near (within a few min) a boundary crossing, but such a change alone proved to be an inadequate or misleading diagnostic in identifying a crossing. If a region was not clearly identifiable as either quiet or disturbed, it was designated "mixed". Henceforth we will refer to these regions as simply Q, M, or D.

We performed a statistical analysis of the data to test quantitatively the consistency of our subjective identifications using as input data the 6 sec averages within fixed 1 min analysis intervals. We obtained distributions and their associated averages and RMS's for F, ϕ, θ, and RMS. These averages and RMS's (based on the 1 min intervals) were finally averaged over the variable lengths of the Q, M, or D regions. This procedure was carried out for a 13-1/2 hour period starting at hour 3 of 5 February 1974. In Figure 6 we show the results for F, ϕ, θ, and two kinds of RMS's defined by

$$\text{CNRMS} = \sqrt{\text{RMS}_x^2 + \text{RMS}_y^2 + \text{RMS}_z^2}/F,$$

the normalized (by F) component-RMS, and

$$\text{FNRMS} = (\text{RMS } [F])/F,$$

the normalized (by F) magnitude-RMS. In the figure X designates a D-region, a thin line is a Q-region, and a thick line denotes an M-region. For comparison, a one-hour interplanetary interval just in front of the bow shock was analyzed similarly and the results are shown by arrows in the far right in the figure. Note the appearance in this representation of the two D-regions shown in Figure 5 at $\sim$ 1200 U.T. and $\sim$1245-1255 U.T.

The relative degree of disturbance for Q vs D as stated above in terms of the region definitions is now immediately obvious, especially for the RMS's. There is a general tendency for F to decrease as we approach the planet, regardless of the region encountered. However, the decrease among the D regions is more marked. We believe that the

general trend is probably influenced predominantly by the strength of the IMF, especially since it appears to decrease, but the marked decrease in the D region field is possibly a result of the interaction of the magnetized solar wind with the planet's ionosphere. The post-encounter interplanetary value of F tends to support the interpretation of the general trend, in as much as it is approximately consistent with a smooth extrapolation of the Q-region values. Considering all parameters in the figure, it appears that the M region is not unique but looks mostly Q-like. It is reasonable to interpret it as being predominantly a Q-region contaminated in some way by being near the D-region at these times.

We now point out some further salient features of Figure 6, starting with the RMS's. For the most part both CNRMS and FNRMS show a consistent and dramatic differentiation between the D and Q/M regions, supporting our subjective identifications of these regions. CNRMS in the Q/M region at $\sim -70\ R_V$ is very nearly equal on average to the IMF value (arrow); this is also true for FNRMS. As we go towards the planet from $-70\ R_V$, the levels of CNRMS or FNRMS in Q/M increase from apparent IMF values to those that might be expected for the near-planet sheath region (cf. Fairfield, 1976). Notice also the non-uniform occurrence-distribution of the D-regions as we go closer to the planet; D-region encounters become more likely and their RMS values increase significantly. The characteristics of this occurrence-distribution virtually eliminate the possibility that all of these structures are simply the signatures solely of IMF events which were convected through the planet's bow shock and eventually past the spacecraft. Interplanetary discontinuities,

for example, are expected to be approximately uniformly distributed on average, although significant variations are observed as shorter time scales are considered (periods of a few days or less).

Excluding the region within $\approx 17\ R_V$ of the planet, the latitude of the field, θ, in the gross sense, appears to vary somewhat smoothly over 70 R_V independent of region-type, as if the measured field is being modulated by the solar wind field. This is also true of the longitude of the field, ϕ, except there is a $\Delta\phi$ of about 35° westward (i.e. clockwise when viewed from above the X_{VO}-Y_{VO} plane), from a Q/M region to a D-region when averaged over all crossings; notice that almost all of the X's in the ϕ panel fall below their Q/M neighbors.

Recall that Figure 6 presents averages usually taken over many mins., and in this form $\Delta\phi$'s across boundaries appear as abrupt changes; the detailed data do not always show such abrupt discontinuities at these boundaries. A complete examination of directional discontinuities at these boundaries and a comparison of them to other discontinuities in the vicinity of Venus will be given in Section 5. The apparent overall modulation of the direction of the measured field by the IMF is in agreement with the interpretation given to the Venusian sheath-like field measured by the Mariner 5 magnetometer (Bridge et al., 1967). As a final comment on the data shown in Figure 6, we note that the spacecraft spent 58% of the 13-1/2 hours in the Q-region, 26% in the M-regions, and only 16% in the D-region.

We have interpreted these statistical results as being consistent with the assumption that the Q-region is a sheath and that the D-region must be a "wake" or wake-like boundary interior to it. However, is it

possible that some subset of the Q-region encounters is not the sheath but is the signature of large scale field line draping around the planet in the sense of a magnetic "comet tail" (cf Ness and Donn, 1966; Wallis, 1967; Dryer, 1970)? If the draped field situation holds, the position vector to Venus from the spacecraft and the magnetic field vector would be parallel (anti-parallel being impossible for the fields actually measured; see Figures 1 and 6). For completeness we examined this hypothesis for both the Q and D regions. Figure 7 shows the superposition of the magnetic field Θ-ϕ angle distributions as shaded areas for the Q (upper panel) and D (lower panel) regions. The key at the bottom of the figure shows the percent occurrence per solid angle element, where an element is $\approx 22^{\circ} \times 22^{\circ}$ at the equator of a panel. N refers to the total number of 6 sec averages employed in the distribution. The crosses give the direction of Venus during the 13-1/2 hour passage. Obviously the results do not support a simple "comet-tail" draped field model. In both the Q and D cases the peak of the field distribution is at least 22° away from the direction of Venus, and the distribution is quite broad, especially for the D-region. In fact, we examined each of the 26 Q- and 19 D-regions separately in this manner and not one individually supported the simple draped model. If such field draping occurs at Venus, it was not evident along Mariner 10's trajectory.

Figure 7 clearly shows a strong tendency of the field to favor the first quandrant in ϕ for the Q regions and the fourth quadrant for the D regions, although the latter distribution is very broad. The split in the ϕ distribution in the Q regions is due to IMF directional changes

seen as delayed sheath field changes at 0728 UT and 1358 UT as Figure 6 shows. In fact, the segment of data between 0728 UT and 1358 UT strongly favors the first quadrant in ϕ, differing from both the previous interval for many (> 19) hours and the subsequent interval up to encounter, over which ϕ primarily assumes the fourth quadrant. Notice that ϕ abruptly swings counterclockwise to the first quadrant at 0728 UT during a Q region transit and remains there throughout the segment for all of the Q regions, while ϕ values for the D regions in the segment appear to track presumably along the large scale IMF direction. This could suggest that in this segment the Q region is a special region distinct from the IMF (or different from a shocked sheath). However, the counterclockwise change in ϕ at 0728 UT was a clear Q → Q directional discontinuity of 78° total angle and the "return" clockwise change in ϕ at 1358 UT was also a clear Q → Q (68° total angle) directional discontinuity.

To interpret Q as an "internal" magnetospheric type of region would require that such large discontinuous field directional changes (as well as many smaller ones) could occur in that region either as rapid changes in time or as (unlikely) spatial features. Temporal changes could perhaps be expected in an induced extended magnetosphere, but it is not likely, considering the magnitude of the components involved, that they would be so sharply discontinuous ($\sim$ 15 sec); they are more characteristic of changes observed in sheath (cf Fairfield, 1976) or IMF measurements. On the other hand, it is not inconceivable that the apparently smoother variation in average ϕ for the D regions only, across the entire 13-1/2 hour period, are somehow related to an induced planetary magnetotail whereby the controlling factor is still the change in the IMF.

We emphasize that the D regions obey the rule that they are clockwise-shifted with respect to their Q/M-region neighbors, with only two exceptions out of 37 crossings. The first exception is at 1403 UT (Figure 6) and the second is at 1615 UT, which should not be unexpected since it apparently is the disturbed sheath discussed in Section 3, and is therefore probably not a conventional D-region.

In an attempt to determine where Mariner 10 first encountered the wake of Venus, many days of pre-encounter were visually inspected. Again this subjective inspection was statistically tested. The results indicate that from ~ hour 20 of 4 February onward (i.e. for $|X_{VO}| \lesssim 100R_V$) the spacecraft was probably encountering Q, M, and D regions according to the criteria defined in association with Figure 5. However, this earlier interval (~ 2000 UT of February 4 to ~ 0300 UT of February 5) is not as clearly delineated according to D or M regions as the later period was. Earlier than hour 20 of 4 February such delineation appears to break down completely, except that some enhancements in fluctuations, via the CNRMS indication, are evident. These regions may be only slightly disturbed, distant sheath and are not unlike locally-disturbed periods seen occasionally in typical IMF data.

Based on these observations over many hours of the pre-encounter period, we estimate that Mariner 10 began to detect a Venus "wake" starting somewhere between 100 and 65 R_V downstream from the planet. The previous preliminary identification of a possibly long magnetic tail at Venus (Ness et al., 1974) was based primarily on the intermittent observation of extremely steady, nearly radially-aligned fields, often of slightly higher magnitude, for periods of up to four hours

beginning on January 28. These fields were oriented toward the general direction of Venus and thus were of the same polarity as the interplanetary field, which was toward the sun (negative sector polarity) during many days pre-encounter. Outside these steady field regions the field direction was variable about the spiral field direction (less radially-aligned), and was clearly less steady in magnitude as well. With observations by a single spacecraft it is impossible to prove or disprove a causal association of these moderately anomalous field regions with Venus. However, both comparisons with the observations nearer to the planet and the post-encounter observations of similar interplanetary periods of steady, nearly radially-aligned fields for several days suggest that it is unlikely that the distant, pre-Venus observations were planet-associated.

5. DISCONTINUITIES IN THE VENUS DOWNSTREAM REGION

Some of the fluctuations seen in the solar wind-Venus interaction region have been found to be magnetic field directional discontinuities (DD's). On the basis of an automatic computer identification of DD's as changes > 30° in the field direction in 42 sec or less [see Sari (1972) for a detailed description of the procedure], there were 22.7 ± 6.2 DD's per day (or slightly less than 1 DD per hour on average) during nine days around the encounter, not including either encounter day itself or the first day post-encounter. The latter was excluded because almost no DD's were observed on that day and was therefore obviously an anomalous day. A total of 44 DD's were counted during the day of encounter, with the distribution peaking during the hour of closest approach (see Figure 4 of Yeates et al., 1977). The encounter

day total DD count is $\geq 3\ \sigma$ above the 9-day average given above. Thus, it is highly probable that at least a substantial fraction of these DD's were generated in the interaction of the solar wind with Venus.

In order to study the characteristics of the Q and D regions observed downstream from the planet in more detail, and in particular to determine whether the wake boundary itself could be characterized as a DD, a fine time-resolution discontinuity analysis was undertaken. A visual survey of 1.2 sec average data identified candidate cases to which a minimum variance analysis (Sonnerup and Cahill, 1967) was applied using the 40 msec data. To insure that the discontinuity plane was well-determined in each case, we required that the intermediate eigenvalue be at least a factor of 4 greater than the eigenvalue associated with the direction of minimum variance ($\lambda_2/\lambda_3 \geq 4$). A total of 29 DD's satisfied this criterion for the period between 0300 and 1600 UT (-70 to -5 R_v). For all except two of these cases the "max to min" eigenvalue ratio, λ_1/λ_3, was greater than 20. The two previously mentioned major rotations of the Q-region field at $\sim$ 0728 UT and $\sim$ 1358 UT were both DD's which satisfied the analysis criterion.

Of the 29 DD's observed in the downstream data over this $\approx$ 13 hour period, 13 were found to occur in the Q (or M) region, 9 in the D region and 7 in close association ($\pm$ 1 min) with the Q-D boundary. There were 25 clearly observed direct transitions between Q and D states. Therefore less than 1/3 of the Q $\rightleftarrows$ D boundary traversals had well-defined DD's associated with them, and most of those did not occur exactly at the boundary as defined by the change in RMS fluctuation levels. This suggests that the DD's were usually associated only with the region of enhanced fluctuations at or adjacent to the boundary and were not a signature of the boundary "surface" itself.

Two successive boundary traversals are shown in the lower part of Figure 8. The D to Q traversal (left) was a broad, structured layer which failed to satisfy the DD analysis criteria. This is typical of the majority of traversals. At the following Q to D transition (right), on the other hand, a relatively sharp DD marked the boundary between the regions, and it was found to be consistent with the magnetic field properties of a tangential discontinuity. [See Burlaga et al. (1977) for definitions of tangential (TD) and rotational (RD) discontinuities and the methods employed in their identification using the magnetic field alone.] The normal component (B_n) was 0.6Y and this component normalized by the average field magnitude ($B_n/\langle B \rangle$) was 0.09. Only two of the 7 boundary-associated DD's had the magnetic characteristics of TD's. The others were identified as RD's.

One of the boundary-associated RD's is seen in the top panel of Figure 8, where one of the early, brief D region observations is shown. In this case the D region was seen for only approximately one minute, with the discontinuity near the center of the interval. In a few cases the transition between regions was seen only as a very gradual onset of fluctuations. An example of this type of transition was shown in the lower panel of Figure 5.

For an assumed constant plasma speed of 400 km/sec, the estimated thickness of the boundary-associated discontinuities ranged between 100 and 5000 km. The thicknesses of DD's that were not close to the boundary traversals were not significantly different in thickness. The normal vector directions computed for the boundary-associated DD's were not consistent with a model of the boundary as a cylindrically-symmetrical

discontinuity surface. However, the latitude angles (θ) of those normals were significantly larger on average than for the non-boundary set ($43^{o} \pm 17^{o}$ compared with $-6^{o} \pm 15^{o}$), and at the spacecraft's locations θ would be large for the normals to an ideal cylindrical surface.

6. SPECTRAL ANALYSIS RESULTS

In order to more completely understand the nature of the magnetic field fluctuations observed during the approach to Venus, the data in selected Q and D regions at various distances from the planet were spectrum-analyzed. The data used in this survey were 1.2 sec averages of the field components and magnitude. This permitted reliable spectra to be computed for time intervals of 10 minutes or greater, making the analysis applicable to a representative sample of both Q and D regions. This restricts the results, however, to the spectral band between 6.9×10^{-3} and 4.2×10^{-1} Hz, corresponding to fluctuations with periods between 144 and 2.4 sec. Power spectral density estimates were computed from finite Fourier transforms of the autocorrelation functions of the respective magnetic field time series (Blackman and Tukey, 1958). Slow trends in the data were removed by subtraction of a second-degree polynomial fit from the measurements.

Figure 9 illustrates the type of results obtained in the study. In order to have representations of vector field fluctuations levels that are independent of specific coordinate frames, we have computed and plotted, at selected frequencies, the trace ($P_x + P_y + P_z$) of the power spectral density matrix. Pairs of typical spectral density curves are shown for both Q and D regions. For comparison, a pair of representative post-encounter interplanetary spectra have been included.

One of the IMF comparison spectra was obtained from a period when the field was relatively undisturbed. The other is typical of periods when fluctuations were present in the field, including coherent waves at several frequencies near 10^{-1} Hz. Both spectra were taken over periods of 15 minutes. From the figure it can be seen that D region power in this spectral band typically can be as much as two orders of magnitude higher than quiet interplanetary levels. Q region spectra, on the other hand, generally lie somewhere between quiet IMF and D region levels, roughly about one order of magnitude above the quiet IMF. The "disturbed IMF" spectrum generally lies below the Q region spectra but crosses over one of them at the low frequency end and the other in the band of frequencies near 10^{-1} Hz where waves were observed. Both the Q and the D region spectra show a characteristic shift of power to higher frequencies nearer to the planet, i.e., there is a crossover of "far" and "near" spectra for both Q and D at a frequency of approximately 2×10^{-2} Hz.

Integrated eigenvalue power values (between 6.9×10^{-3} and 4.2×10^{-1} Hz) were used to compute anisotropy (maximum to minimum) ratios. A comparison between adjacent Q and D regions suggests that D region fluctuations were generally of similar anisotropy to the Q region fluctuations, with ratios typically between 3 and 7. Spectral and plane wave analysis (Fowler et al., 1967; Rankin and Kurtz, 1970) of the detailed 40 msec measurements over one minute intervals has shown that there were at times coherent waves in both Q and D regions up to a doppler-shifted frequency of 0.6 Hz. These were left-hand nearly circularly polarized waves similar in characteristics to waves observed by Mariner 10 in both the interplanetary medium (Behannon, 1976) and

Mercury's magnetosheath (Fairfield and Behannon, 1976), where they were postulated to be ion cyclotron waves. Similar waves were observed occasionally near a frequency of 0.3 Hz in Q regions only.

On the basis of the power spectral studies we conclude that the Q and D regions are generally similar in fluctuation characteristics, except that there is roughly an order of magnitude more power in D region fluctuations than in those found in Q regions. In this respect the Q regions most closely resemble "disturbed" IMF.

7. SUMMARY AND CONCLUSIONS

Our analysis has been concerned primarily with the down-stream region of the solar wind-Venus interaction. During at least the two days prior to closest approach the spacecraft encountered two distinct regions and occa[illegible] mixture of the two. These regions have been referred to as quiet (Q), disturbed (D) and mixed (M). (Observations prior to this period show that the spacecraft was in either the Q-region or the interplanetary medium almost exclusively.) We now summarize reasons for believing the Q-region to be sheath created by the solar wind-planet interaction.

1) None of the boundary crossings observed downstream from Venus have the characteristics of bow shock crossings, either in the general field signature or in terms of satisfying the plasma-field conservation conditions (K. Ogilvie, private communication). Therefore, the spacecraft never encountered the bow shock until after closest approach. If the shock existed throughout the extended encounter period, then presumably it was located outside the location of the spacecraft approach trajectory. Since Mariner 10 was within the probable shock position but well outside

the geometrical shadow region during most of the approach period, and since the observations show that most of this time was spent in the Q or M regions (84%) but with the Q/M-region observed less frequently closer to the planet, it is not unreasonable to associate the Q-region with a sheath region.

2) The Q-region has a general magnetic appearance consistent with a sheath-like region from visual inspection of 6 sec average data (Figure 5), from spectral analysis (Figure 9) and from the characteristics exhibited by the statistical fluctuation parameters CNRMS and FNRMS (Figure 6). The spectra show that there is generally a higher power spectral density in the Q-region than in the undisturbed IMF. Q-region CNRMS and FNRMS values approach IMF values at increasingly greater distances downstream from the planet. By contrast, the D-region values of these parameters are significantly higher nearer the planet than Q-region values and remain enhanced relative to IMF levels at significant distances ($\sim$ 70 R_V or farther) from Venus.

3) The electron-plasma properties of the Q-region are at least qualitatively consistent with its identification as a sheath region (Yeates et al., 1977).

4) The approximately cylindrically-symmetrical orientation of the near-planet field was not consistent with a typically magnetotail-like geometry. It is at least plausible that it could have been produced by the necessity for the sheath field to avoid the approximately spherical ionospheric obstacle to solar wind flow. A similar reconfiguration is seen in the magnetosheath field in the vicinity of the earth's magnetopause (Fairfield, 1976).

The D-region data associated with the observed boundary crossings suggest the existence interior to the Q-region of a quasi-turbulent region that can be either a boundary layer or a broader disturbed region and either continuous in time, but fluctuating in position, or intermittent in time. Accordingly, then, we interpret the D-region encounters as periods when the spacecraft was passing into a planetary wake or wake-like boundary layer or region. These terms are used here in a general sense, meaning that the boundary is either a zone enclosing a true quasi-static wake or is an approximately cone-shaped surface within which there is a high probability that transient convected disturbed plasma will occur. Since no previous spacecraft has encountered the Venusian "far wake" and since Mariner 10 did not enjoy the advantage of comparison with simultaneous, near-Venus interplanetary data, choosing confidently between the steady-state or transient interpretations is probably impossible. Equally difficult, from a single spacecraft's data, is choosing between a transient large-scale wake and a time-varying wake, consisting of parcels of plasma tearing away from the Venusian atmosphere/ionosphere, for example. However, to accept the steady-state model requires believing that the spacecraft was closely skimming along the wake boundary during the day previous to encounter, because at no time did it obviously experience deep penetration into the steady-state wake proper. That is, there was no extended period (> 16 min) of disturbed fields observed during the approach to Venus.

From the signatures of the magnetic field observations alone we estimate that Mariner 10 did not encounter Venus-related plasma

earlier than approximately hour 20 of 4 February, when it was $\approx 100\ R_V$ from Venus. Conservatively then the data are consistent with a "wake" (when it is present) of at least that length. The preliminary report of a possibly much longer "wake" or "tail" (Ness et al., 1974) was based on the sporadic observation for > 6 days prior to encounter of fields which appeared to be atypical of interplanetary conditions but which with only one spacecraft cannot be unambiguously attributed to the solar-wind-Venus interaction.

Figure 10 shows a schematic view of the region downstream of Venus with regard to its probable state and geometry; qualitative comments on the properties of the electron-plasma (K. Ogilvie, private communication) and magnetic field for the two principal regions are shown, along with black boxes on the trajectory indicating the D-region encounters. The last D-region is probably disturbed sheath as discussed in Section 3 (cf. Greenstadt, 1971). The shaded "wake" is meant to suggest simply that the conical region shown interior to the Mariner 10 trajectory contained planet-associated plasma ither continuously during the observing period or sporadically as a result of a transient interaction process. However, since the region was apparently not penetrated deeply it cannot be demonstrated that the observed "disturbed" plasma filled the entire conical volume. In fact, the description of the wake as a "magnetically disturbed, hotter, slower, and less dense plasma" also qualitatively describes the geomagnetic tail-boundary layer with respect to the earth's magnetosheath which is cooler, faster and more dense. Although not unique to a boundary layer description, such characteristics lend credence to the possibility.

On the other hand, on the basis of both theoretical calculations and inferences from measurements by Mariner 5 and Veneras 4, 9 and 10, Perez de Tejada and Dryer (1976) and Perez de Tejada et al. (1977) have concluded that the region of mixing between solar wind and ionospheric plasma converges toward the wake axis within a short distance downstream from Venus. They suggest that downstream of a position approximately 2 R_v behind the planet along the sun-Venus line the entire cross-section of the tail may be affected by the mixing process, although the geometry of such a viscous interaction process could be significantly altered by the presence of even a weak planetary magnetic field, either intrinsic or induced.

One of the most interesting observations connected with the discovery of a Venus wake, either steady or transient, is the persistent clockwise shift in the ϕ-angle of the field observed in crossing from Q to D-regions. The spacecraft certainly did not experience an Earth-like magnetosphere, but there is the remote possibility that a pseudomagnetosphere engulfing the planet could be responsible for the observed ϕ shifts. All attempts to explain this clockwise shift of field in terms of gradients in convected fields or long range field-draping around the planet have failed, partly because the shift occurs regardless of the quadrant of the Q-region ϕ angle, either first or fourth. If the observations of clockwise shifts in ϕ across Q → D boundaries are indicative of entry into a planetary tail field region, then that field appears to have a <u>significant</u> and <u>negative</u> Y component for most of the traversals, especially when seen on a fine (6 sec) time scale. Such a large cross-tail component does not appear to be generally consistent with a

magnetotail type of configuration. Furthermore, the field observed by Mariner 10 had a polarity (i.e. the sign of the X component predominantly) which was inconsistent with that expected from the dipole sense inferred by Russell (1976a); this is also true of the sign of the significant Y component if aberration due to planetary motion is considered. However, Russell's (1976b) description of a possible Venusian magnetotail did not include positions as far from the planet-sun line as the Mariner 10 trajectory. Dolginov (1976) concluded from Venera 9 and Mariner 5 observations that the near planet "tail-field" apparently has a variable polarity, which could imply an induced planetary field. However, a more recent and more extensive analysis of Venera 9 and 10 data (Dolginov et al., 1977) provides some support for the view that two lobes of opposite magnetic polarity, separated by a thin neutral sheet region, were observed in the near-planet downstream region over an extended period of time, but with considerable variability in detailed geometry.

Since attempts to explain the Q → D clockwise field direction shift observed along the Mariner 10 trajectory as an effect of the planetary interaction have not been successful, the suggestion by Yeates et al., (1977) is intriguing. They have developed a model for the disturbed regions (which coincide for the most part with our D regions) that depends on a specific direction of the impinging IMF as a cause, in conjunction with the presence of the planet and its ionosphere as an obstacle to solar wind flow. In particular, to explain the existence of the D-regions they suggest a plasma instability (Wu and Davidson, 1972; Hartle and Wu, 1973) that requires the field to be perpendicular to the plasma

flow direction, which is approximately along $-\hat{X}_{VO}$. In this connection, we examined the field for 11 days before and 6 days after encounter to see how frequently $\alpha \approx 90^{o}$, where $\alpha = \cos^{-1}(B_x/B)$, i.e., α is the cone-angle of a cone with axis along $\hat{X}_{VO}$. Figure 11 shows the results in terms of the percent occurrence of $\vec{B}$ perpendicular to $\hat{X}_{VO}$, based on 6 sec averages taken in three-hour intervals for two different criteria (see the key in the figure) that represent allowable ranges for α. The most important feature of the profile is its uniformity, i.e., the closest approach to Venus does not mark a strongly significant change in the occurrence of $\vec{B}$ perpendicular to $\hat{X}_{VO}$ at this time, and the choice of criterion is not significant (others were also used). However, minor aberrations appear late on February 7 and on February 10, i.e. during the IMF portion when the occurrences are fewer (the periods of low % include those periods in which the previously reported radially aligned fields were observed).

The overall profile of these data seems to imply that the condition $\alpha \approx 90^{o}$ was generally rather frequently satisfied during this entire period, and that the shifts in ϕ-direction that occurred in the pre-encounter period may plausibly be causally associated with IMF direction changes rather than produced by the solar wind-Venus interaction. The higher levels of fluctuations inside the D-regions may, however, be produced by the interaction either directly or indirectly via instabilities.

A significantly larger number of directional discontinuities were seen on the day of encounter than the occurrence totals found on adjacent days (Figure 4 of Yeates et al., 1977), but only on a relatively small number (28%) of the observed Q $\rightleftarrows$ D boundary traversals were rigorously

identifiable DD's found to be occurring in close association with the boundary. The characteristics of these boundary-associated DD's were mixed, however, and similar to those found in general in either the Q or D-region.

Thus, the results of the analysis of magnetic fields in the downstream region of the solar-wind-Venus interaction are consistent with the interpretation of Yeates et al. (1977) but, we believe, also allow for the possibility of a steady-state wake that occasionally "flaps" or changes configuration in response to changes in the IMF and solar wind.

ACKNOWLEDGEMENTS

We wish to thank Dr. N. F. Ness, J. K. Alexander and Dr. Y. C. Whang for helpful criticism. We are grateful to Drs. K. Ogilvie and C. Yeates of the Mariner 10 plasma team for providing added insight into the problem through free access to their electron-plasma data and for their comments. We thank M. Silverstein and W. Mish for computer programming assistance. We also thank Drs. M. Dryer and H. Perez de Tejada for helpful comments on the interpretation of the observations.

REFERENCES

Bauer, S. J., L. H. Brace, D. M. Hunter, D. S. Intriligator, W.C. Knudsen, A.F. Nagy, C.T. Russell, F.L. Scarf, and J.H. Wolfe, The Venus ionosphere and solar wind interaction, Space Sci. Rev., 20, 413, 1977. (See also other articles in this special Venus Exploration Issue.)

Behannon, K.W., Observations of the interplanetary magnetic field between 0.46 and 1 A.U. by the Mariner 10 spacecraft, Ph.D. Thesis, Catholic University of America, NASA-GSFC X-692-76-2, January 1976.

Behannon, K.W., and F.W. Ottens, Mariner 10 interplanetary magnetic field measurements November 1973-March 1974, NASA-GSFC X-692-76-208, September 1976.

Blackman, R.B., and J.W. Tukey, The measurement of power spectra, Dover, New York, 1958.

Bridge, H.S., A.J. Lazarus, J.D. Scudder, K.W. Ogilvie, R.E. Hartle, J.R. Asbridge, S.J. Bame, W.C. Feldman, and G.L. Siscoe, Observations at Venus encounter by the plasma experiment on Mariner 10, Science, 183, 1293, 1974.

Bridge, H.S., A.J. Lazarus, C.W. Snyder, E.J. Smith, L. Davis, Jr., P.J. Coleman, Jr., and D. E. Jones, Mariner V: Plasma and magnetic fields observed near Venus, Science, 158, 1669, 1967.

Burlaga, L.F., J.F. Lemaire, and J. M. Turner, Interplanetary current sheets at 1 A.U., J. Geophys. Res., 82, 3191, 1977.

Dolginov, Sh.Sh., Planetary magnetism and dynamo mechanism problem, USSR Academy of Sciences preprint No. 15a, Moscow, 1976.

Dolginov, Sh.Sh., E.G. Eroshenko, and L. Lewis, Nature of the magnetic field in the neighborhood of Venus, translated from Kosmicheskie Issledovaniya, 7, No. 5, pp. 747-752, Plenum Pub. Co., Sept.-Oct. 1969.

Dolginov, Sh.Sh., E.G. Eroshenko, and L.N. Zhuzgov, Magnetic field investigation with interplanetary station "Venera-4", translated from Kosmicheskie Issledovaniya, 6, No. 4, pp. 561-575, Plenum Pub. Co., July-Aug. 1968.

Dolginov, Sh.Sh., E.G. Eroshenko, L.N. Zhuzgov, V.B. Buzin, and V.A. Sharova, Preliminary results of magnetic field measurements at pericenter region of "Venera 9" orbit, translation Soviet Astron. Letters, 2, 34, 1976.

Dolginov, Sh.Sh., Y.G. Yeroshenko, L.N. Khuzgov, V.A. Sharova, and V.B. Buzin, Magnetic fields in the close vicinity of Venus according to the Venera 9 and 10 data, Institute of Terrestrial Magnetism, Ionosphere and Radiowave Propagation, Moscow, USSR, preprint, IAGA/IAMAP Joint Assembly, Seattle, 1977.

Dryer, M., Solar wind interactions-hypersonic analogue, Cosmic Electrodyn. 1, 115, 1970.

Dryer, M., and G.R. Heckman, On the hypersonic analogue as applied to planetary interaction with the solar plasma, Planet. Space Sci., 15, 515, 1967.

Fairfield, D.H., Magnetic field of the magnetosheath, Rev. Geophys. Space Phys., 14, 117, 1976.

Fairfield, D.H., and K.W. Behannon, Bow shock and magnetosheath waves at Mercury, J. Geophys. Res., 81, 3897, 1976.

Fowler, R.A., B.J. Kotick, and R.D. Elliot, Polarization analysis of natural and artifically induced geomagnetic micropulsations, J. Geophys. Res. 72, 2871, 1967.

Greenstadt, E.W., Dependence of shock structure at Venus and Mars on orientation of the interplanetary magnetic field, Cosmic Electrodyn. 1, 380, 1971.

Greenstadt, E.W., I.M. Green, G.T. Inouye, D.S. Colburn, J.H. Binsack, and E.F. Lyon, Dual satellite observations of Earth's bow shock, Cosmic Electrodyn., 1, 160, 1970.

Greenstadt, E.W., I.M. Green, G.T. Inouye, A.J. Hundhausen, S.J. Bame, and J.B. Strong, Correlated magnetic field and plasma observations of the Earth's bow shock, J. Geophys. Res., 73, 51, 1968.

Hartle, R.E., and C.S. Wu, Effects of electrostatic instabilities on planetary and interstellar ions in the solar wind, J. Geophys. Res., 78, 5802, 1973.

Lepping, R.P., K.W. Behannon, and D.R. Howell, A method of estimating zero level offsets for a dual magnetometer with flipper on a slowly rolling spacecraft: application to Mariner 10, NASA-GSFC X-692-75-268, October 1975.

Lepping, R.P., K.W. Behannon, and D. R. Howell, Mariner 10 near-Venus magnetic field and trajectory data with bibliography, NASA-GSFC X-695-77-207, August 1977.

Ness, N.F., Is there any evidence for a magnetic field of Venus?, NASA-GSFC X-690-76-78, April 1976.

Ness, N.F., Comment on "The Venus bow shock, detached or attached?" by C.T. Russell, J. Geophys. Res., 82, 2439, 1977.

Ness, N.F., K.W. Behannon, R.P. Lepping, and K.H. Schatten, Use of two magnetometers for magnetic field measurements on a spacecraft, J. Geophys. Res., 76, 3564, 1971.

Ness, N.F., K.W. Behannon, R.P. Lepping, Y.C. Whang, and K.H. Schatten, Magnetic field observations near Venus: preliminary results from Mariner 10, Science, 183, 1301, 1974.

Ness, N.F., and B.D. Donn, Concerning a new theory of type I comet tails, Nature et Origine des Cometes, Proceedings of the 13th International Astrophysical Symposium at Liege, Belgium, July 1965, p. 343, 1966.

Perez de Tejada, H., and M. Dryer, Viscous boundary layer for the Venusian ionopause, J. Geophys. Res., 81, 2023, 1976.

Perez de Tejada, H., M. Dryer, and O.L. Vaisberg, Viscous flow in the near-Venusian plasma wake, J. Geophys. Res., 82, 2837, 1977.

Rankin, D. and R. Kurtz, Statistical study of micropulsation polarizations, J. Geophys. Res., 75, 5444, 1970.

Rizzi, A.W., Solar wind flow past the planets Earth, Mars, and Venus, Ph.D. dissertation, 211 pp., Stanford Univ., Stanford, Calif., 1972.

Russell, C.T., The magnetic moment of Venus: Venera 4 measurements reinterpreted, Geophys. Res. Lett., 3, 125, 1976a.

Russell, C.T., The magnetosphere of Venus: evidence for a boundary layer and a magnetotail, Geophys. Res. Lett., 3, 589, 1976b.

Russell, C.T., The Venus bow shock: detached or attached?, J. Geophys. Res., 82, 625, 1977a.

Russell, C.T., Reply, J. Geophys. Res., 82, 2441, 1977b.

Sari, J.W., Modulation of low energy cosmic rays, Ph.D. dissertation Univ. of Maryland, NASA-GSFC X-692-72-309, August 1972.

Seek, J.B., J.L. Scheifele, and N.F. Ness, GSFC Magnetic Field Experiment: Mariner 10, NASA-GSFC X-695-77-256, October 1977.

Siscoe, G.L., Towards a comparative theory of magnetospheres, preprint, to appear in Solar System Plasma Physics-A Twentieth Anniversary Review, eds: C.F. Kennel, L.J. Lanzerotti and E.N. Parker, North-Holland Pub. Co., 1977.

Sonnerup, B.U.O., and L.J. Cahill, Jr., Magnetopause structure and attitude from Explorer 12 observations, J. Geophys. Res., 72, 171, 1967.

Spreiter, J.R., Magnetohydrodynamic and gasdynamic aspects of solar-wind flow around terrestrial planets: a critical review, Proceedings of US-USSR Bilateral Seminar, Moscow, Nov. 17-21, 1975, NASA SP-397, 135, 1976.

Villante, U., Evidence for a bow shock structure at $\sim 400\ R_E$: Pioneer 7, J. Geophys. Res., 81, 1441, 1976.

Wallis, M., Comet tail streamers in the solar wind, Planet. Space Sci., 15, 137, 1967.

Whang, Y.C., N.F. Ness, K.W. Behannon, and R.P. Lepping, Solar wind-Venus interaction observed from magnetic field experiment on Mariner 10, Solar Wind Three, Ed. C.T. Russell, Inst. Geophys. and Planetary Phys., UCLA, p. 428, July 1974.

Wu, C.S., and R.C. Davidson, Electromagnetic instabilities produced by neutral particle ionization in interplanetary space, J. Geophys. Res., 77, 5399, 1972.

Yeates, C., K.W. Ogilvie, and G. Siscoe, Plasma electron observations in the wake of Venus, to be published, J. Geophys. Res., 1977.

FIGURE CAPTIONS

Figure 1 The Mariner 10 trajectory for approximately 14 hours before closest approach to Venus in VO coordinates (see text). The black boxes along the trajectory denote periods when wake or wake boundary layer fields were probably observed.

Figure 2 Mariner 10 6-sec average magnetic field data and associated trajectory (in cylindrical coordinates - see text) for ~ 7-1/2 hours. Note the contrasting "quiet" and "disturbed" regions observed downstream from the planet. See Figure 5 for an expanded view of the observations near 1200 and 1300 UT.

Figure 3 Magnetic field characteristics in the near-Venus region. The angles ω_B and ω_T are associated with the observed field orientation and the spacecraft position, respectively, and are defined both in the text and in Figure 4. When the two angles are equal, the measured field is tangent to a cylindrical surface.

Figure 4 The definitions of the angles ω_B and ω_T measured in the Y-Z plane; ω_B is the colatitude of the field and ω_T is the latitude of the spacecraft position projected onto that plane.

Figure 5 Examples of typical quiet (Q), mixed (M), and disturbed (D) magnetic field regions downstream of Venus (top panel) and detailed data (40 msec sample period) showing a quiet to disturbed traversal (bottom panel).

Figure 6 Average and statistical properties of the magnetic field for 13-1/2 hours pre-encounter; thin lines represent Q-regions, thick lines denote M-regions, and X's indicate D-regions. Multiple X's at a fixed level indicate the length of a single D-region. The arrows at far right represent post-Venus IMF values.

Figure 7 Directional distributions of the magnetic field in terms of its VO-coordinate latitude (θ) and longitude (ϕ) over the 13-1/2 hour period described in Figure 6. Crosses on the far right and left span the locations of Mariner 10 during this period.

Figure 8 Detailed (40 msec sample period) magnetic field data showing examples of Q $\rightleftarrows$ D crossings. The top panel shows a D-region, lasting for $\sim$ 1 min, in the middle of which a rotational discontinuity occurred. In the bottom panel on the left is shown a relatively broad D $\rightarrow$ Q transition with no directional discontinuity in the minimum variance sense. The bottom panel, right, shows a Q $\rightarrow$ D transition which is rather sharply defined by a tangential discontinuity. A continuous D-region occurred from $\sim$ 1508:05 to 1512:20 U.T.

Figure 9 Power spectral density traces of the magnetic field for representative intervals on encounter day, both upstream and downstream of the planet.

Figure 10 A schematic representation of the plasma "wake" and bow shock of Venus in relation to the Mariner 10 trajectory, all in cylindrical coordinates. The qualitative properties of the plasma in the contrasting regions are also given (Ogilvie, private communication). As in Figure 1, D-regions are shown as black boxes along the trajectory.

Figure 11 The percent occurrence of $\vec{B}$ perpendicular to $\hat{X}_{VO}$ for 17 days around encounter based on 6 sec averages over 3 hour periods.

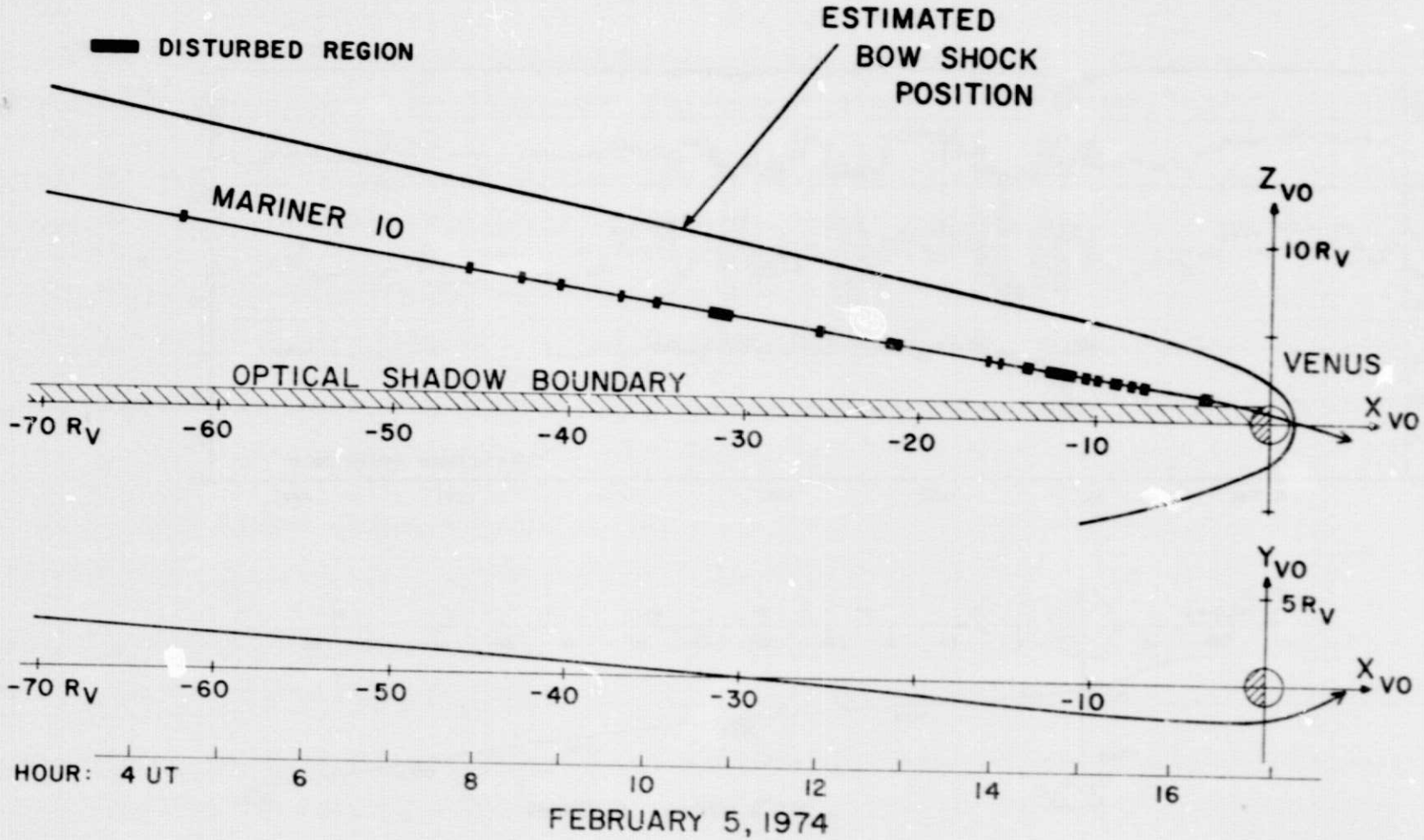
DISTURBED REGION
ESTIMATED
BOW SHOCK
POSITION
MARINER 10
OPTICAL SHADOW BOUNDARY
Z VO
10 RV
VENUS
X VO
-70 RV
-60
-50
-40
-30
-20
-10
Y VO
5 RV
X VO
-70 RV
-60
-50
-40
-30
-10
HOUR: 4 UT
6
8
10
12
14
16
FEBRUARY 5, 1974

Figure 1

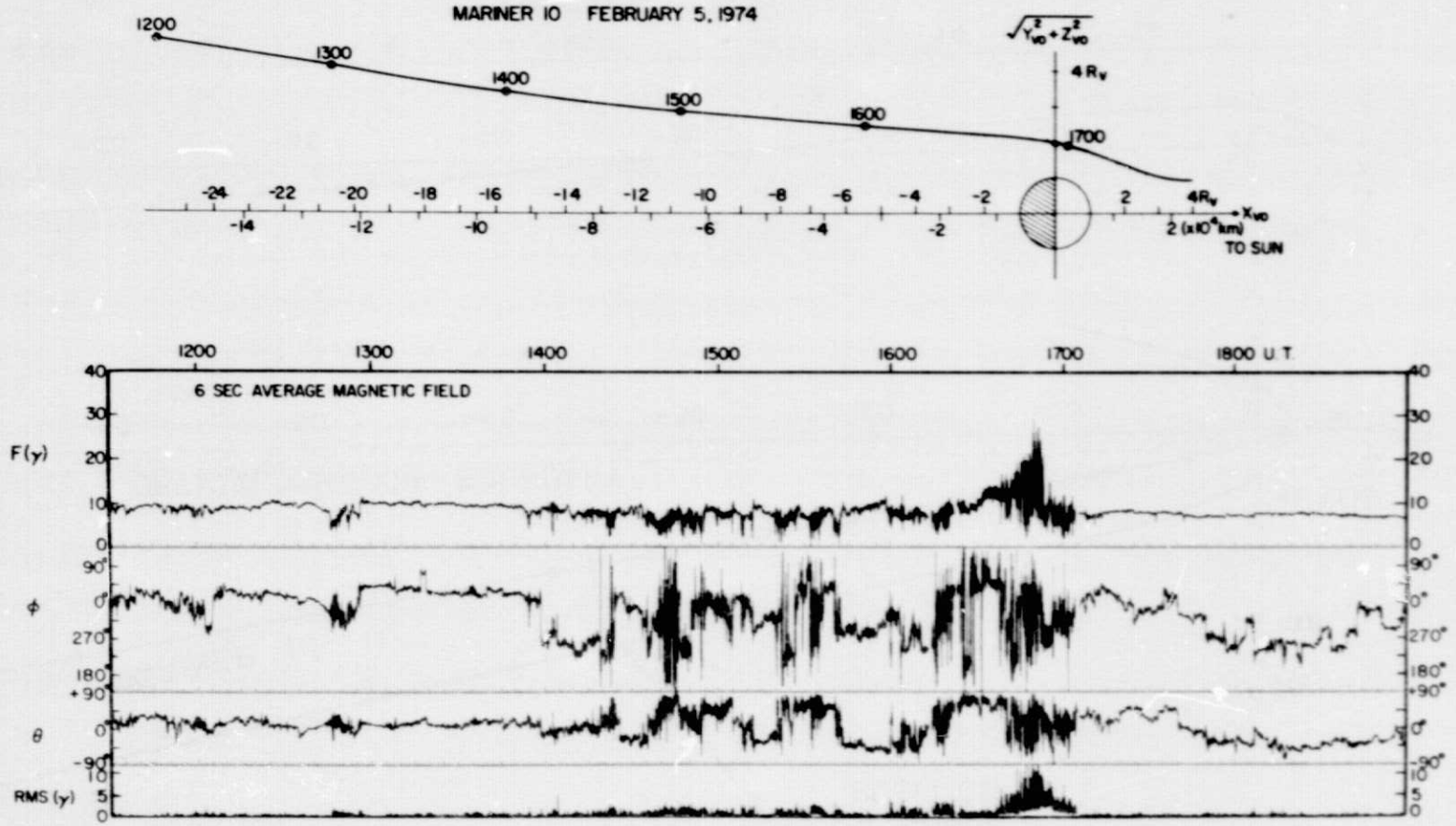
MARINER 10 FEBRUARY 5, 1974
1200
1300
1400
1500
1600
1700
$\sqrt{Y_{VO}^2 + Z_{VO}^2}$
4 R_V
-24 -22 -20 -18 -16 -14 -12 -10 -8 -6 -4 -2 2 4R_V X_{VO}
-14 -12 -10 -8 -6 -4 -2 2 ($\times 10^4$ km)
TO SUN
1200 1300 1400 1500 1600 1700 1800 U.T.
6 SEC AVERAGE MAGNETIC FIELD
F(y)
40 30 20 10 0
ϕ
90° 0° 270° 180°
θ
+90° 0° -90°
RMS (y)
10 5 0

Figure 2

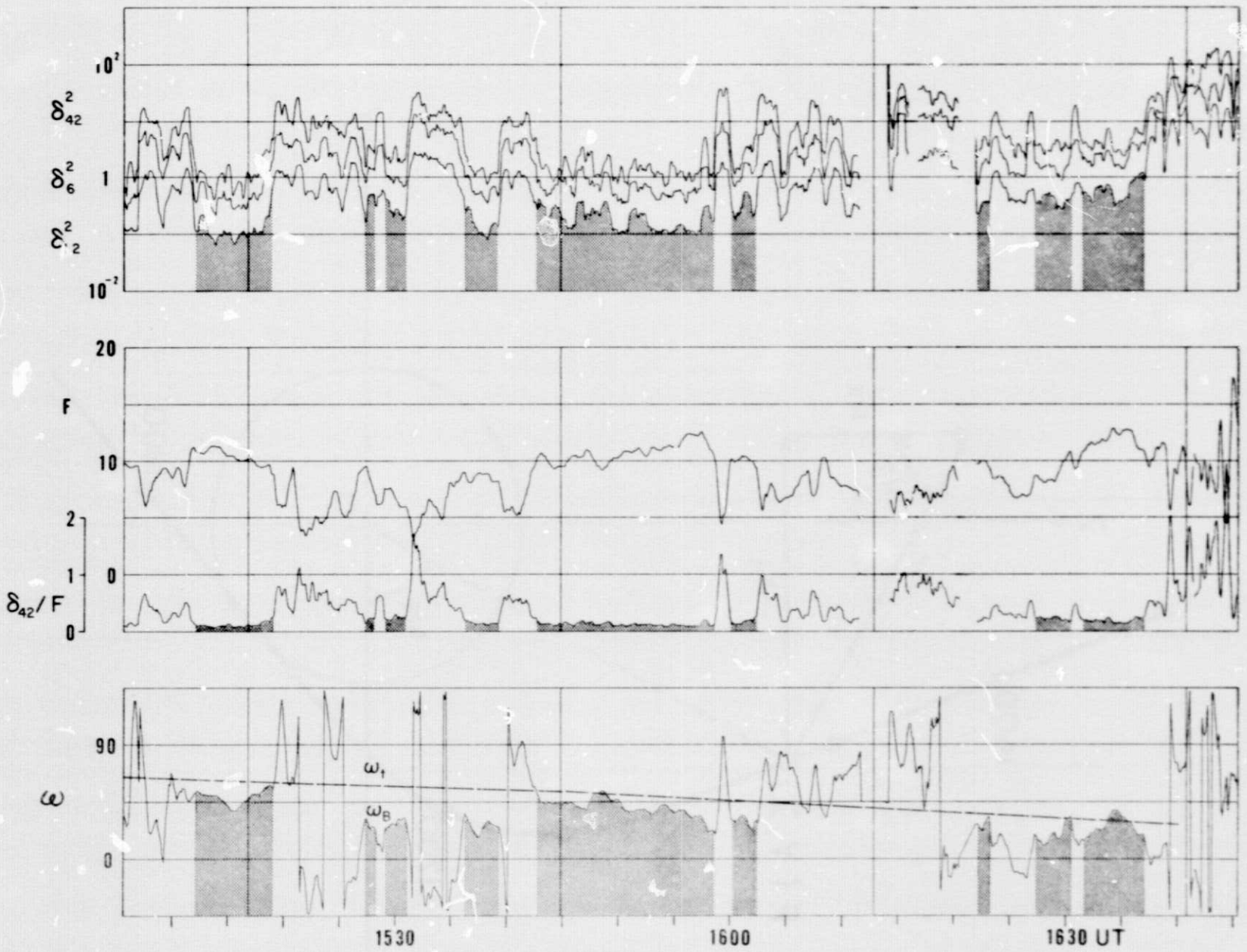
10^2
δ^2_{42}
δ^2_6
1
δ^2_{12}
10^{-2}
20
F
10
2
1
0
δ_{42}/F
0
90
ω
ω_t
ω_B
0
1530
1600
1630 UT
5 FEBRUARY 1974

Figure 3

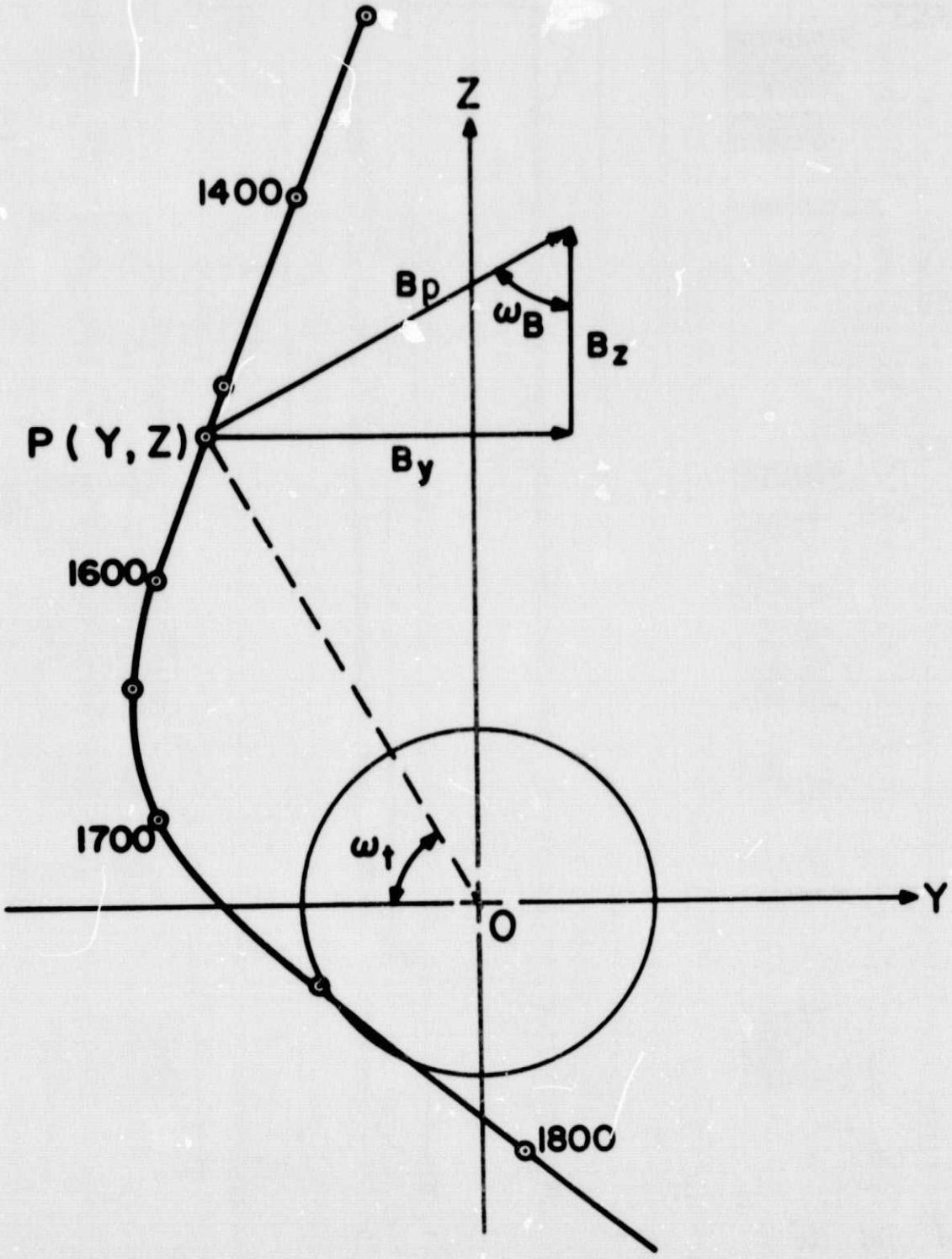

Figure 4

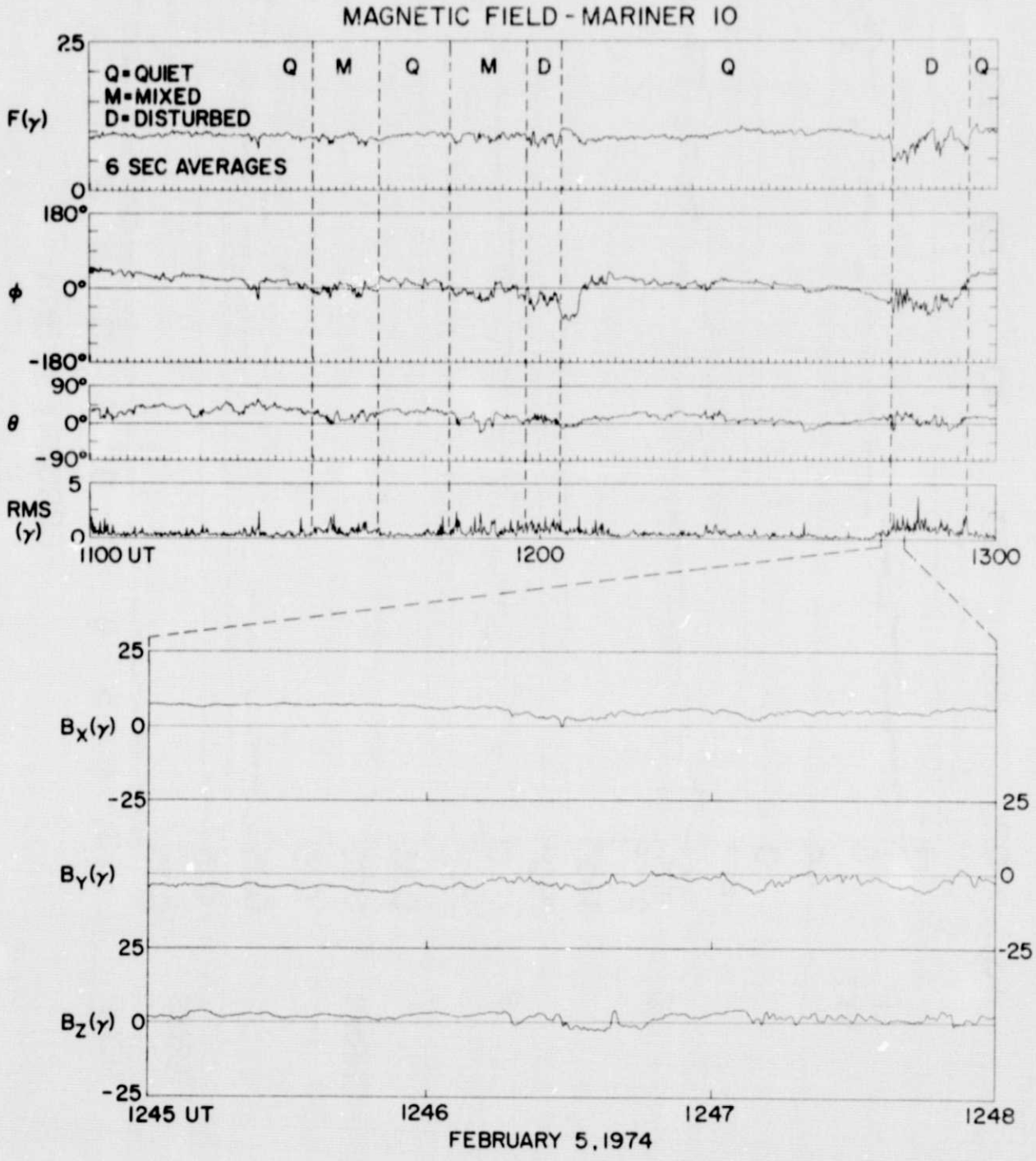
MAGNETIC FIELD - MARINER 10
Q = QUIET
M = MIXED
D = DISTURBED
6 SEC AVERAGES
Q M Q M D Q D Q
F(γ)
25
0
φ
180°
0°
-180°
θ
90°
0°
-90°
RMS (γ)
5
0
1100 UT
1200
1300
$B_X(\gamma)$
$B_Y(\gamma)$
$B_Z(\gamma)$
25
0
-25
1245 UT
1246
1247
1248
FEBRUARY 5, 1974

Figure 5

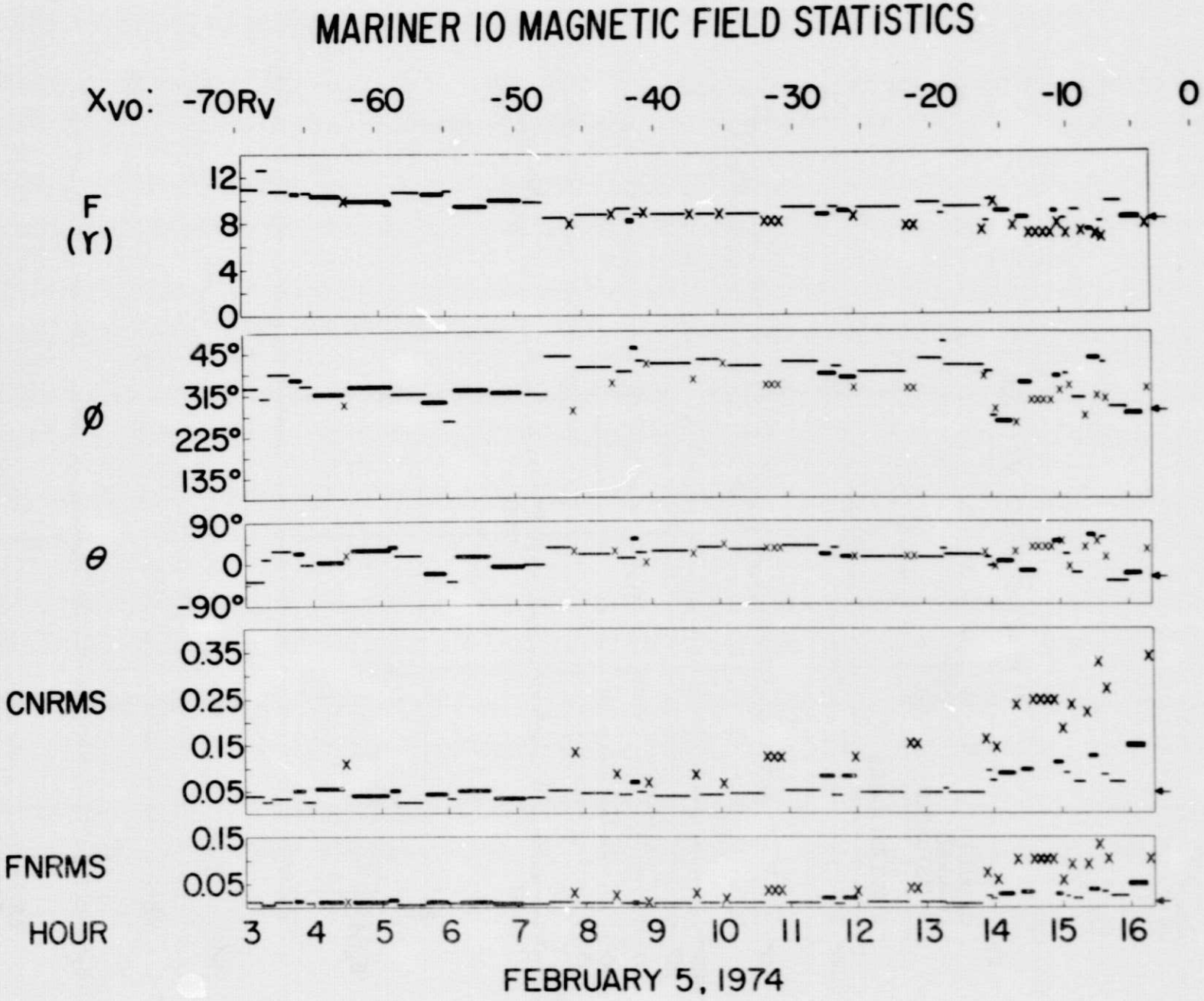
MARINER 10 MAGNETIC FIELD STATISTICS
X_{VO}: -70Rv -60 -50 -40 -30 -20 -10 0
F (γ)
12
8
4
0
ø
45°
315°
225°
135°
θ
90°
0
-90°
CNRMS
0.35
0.25
0.15
0.05
FNRMS
0.15
0.05
HOUR
3 4 5 6 7 8 9 10 11 12 13 14 15 16
FEBRUARY 5, 1974

Figure 6

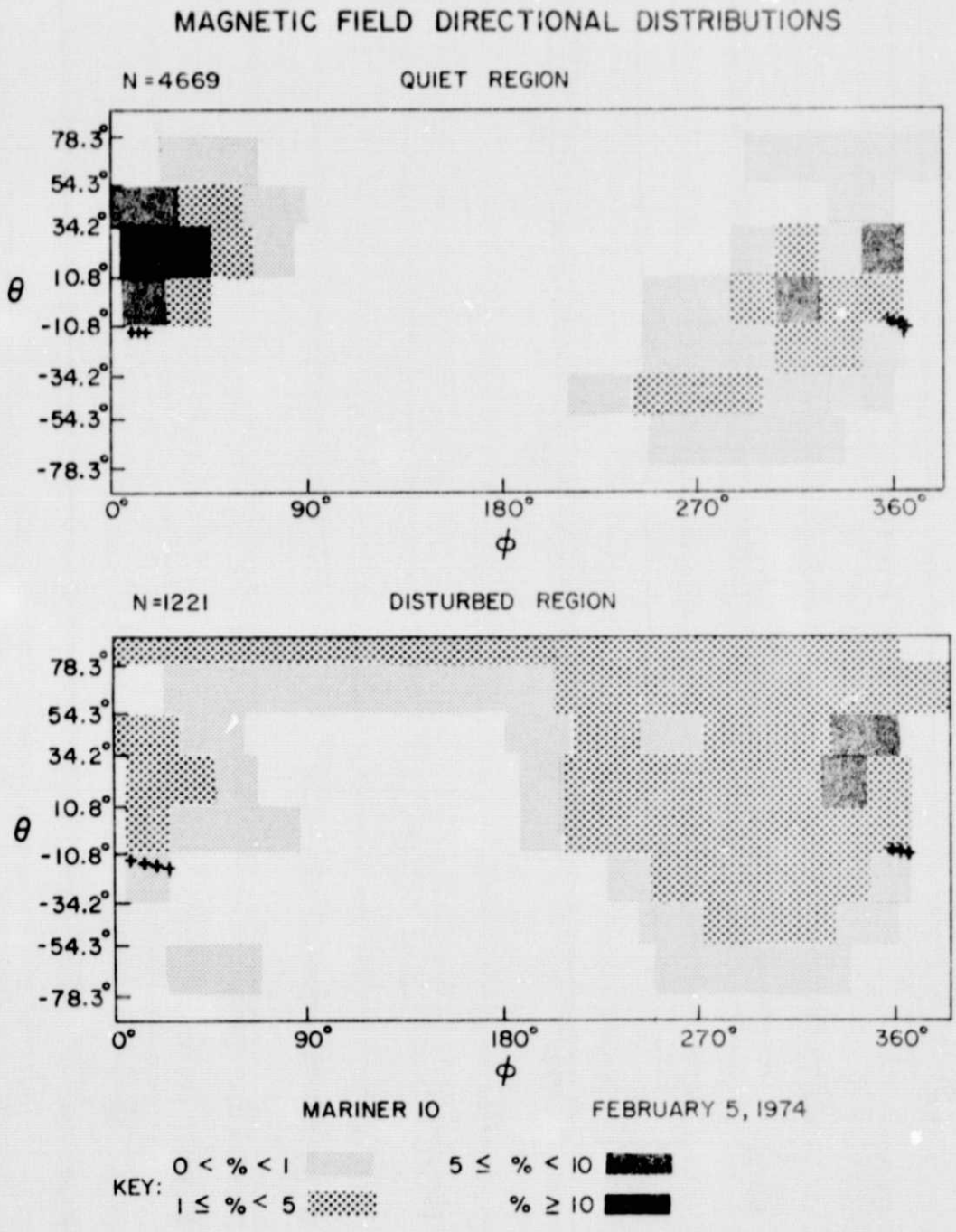
MAGNETIC FIELD DIRECTIONAL DISTRIBUTIONS
N = 4669
QUIET REGION
78.3°
54.3°
34.2°
10.8°
-10.8°
-34.2°
-54.3°
-78.3°
θ
0°
90°
180°
270°
360°
φ
N = 1221
DISTURBED REGION
78.3°
54.3°
34.2°
10.8°
-10.8°
-34.2°
-54.3°
-78.3°
θ
0°
90°
180°
270°
360°
φ
MARINER 10
FEBRUARY 5, 1974
KEY:
0 < % < 1
1 ≤ % < 5
5 ≤ % < 10
% ≥ 10

Figure 7

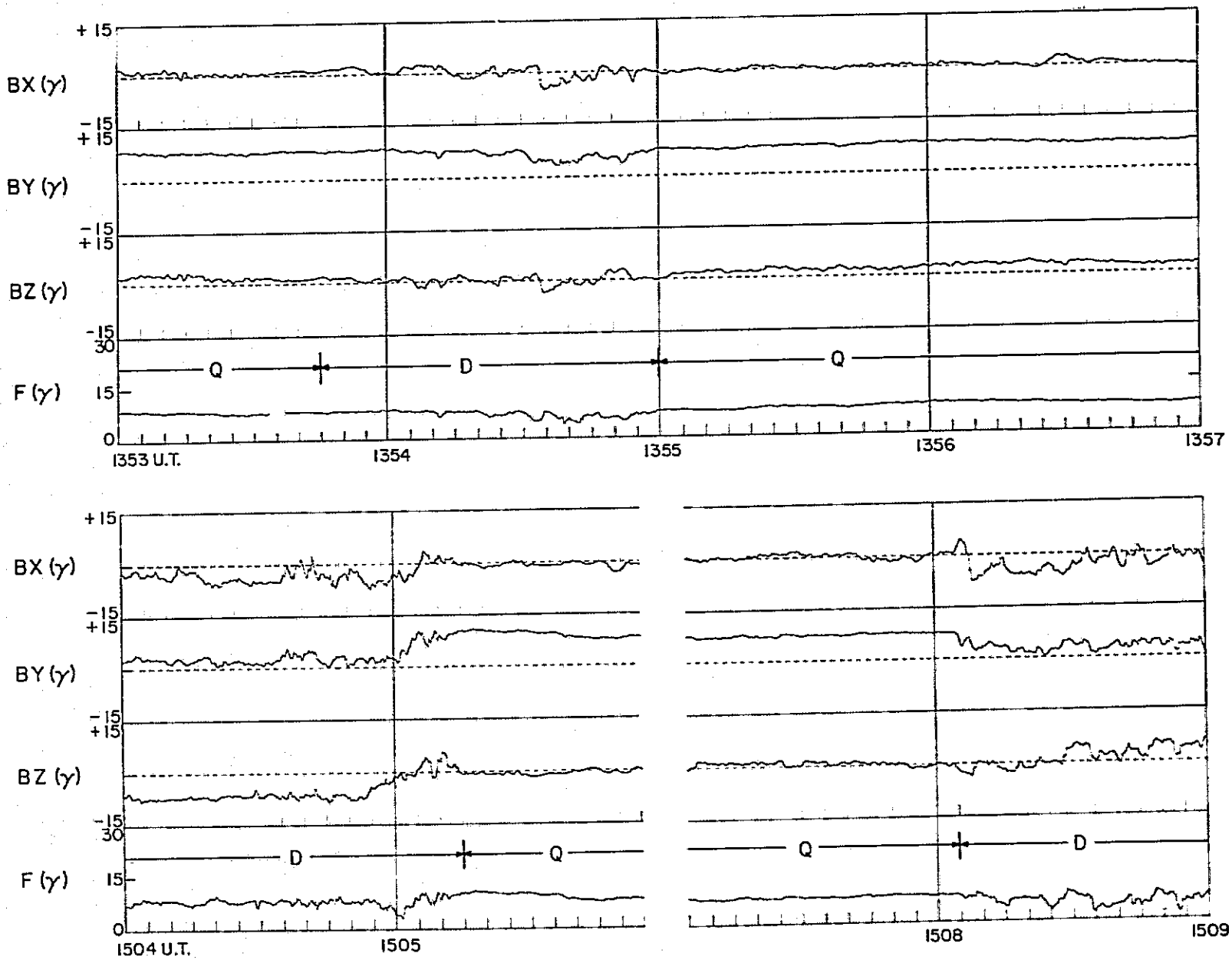

FEBRUARY 5, 1974

Figure 8

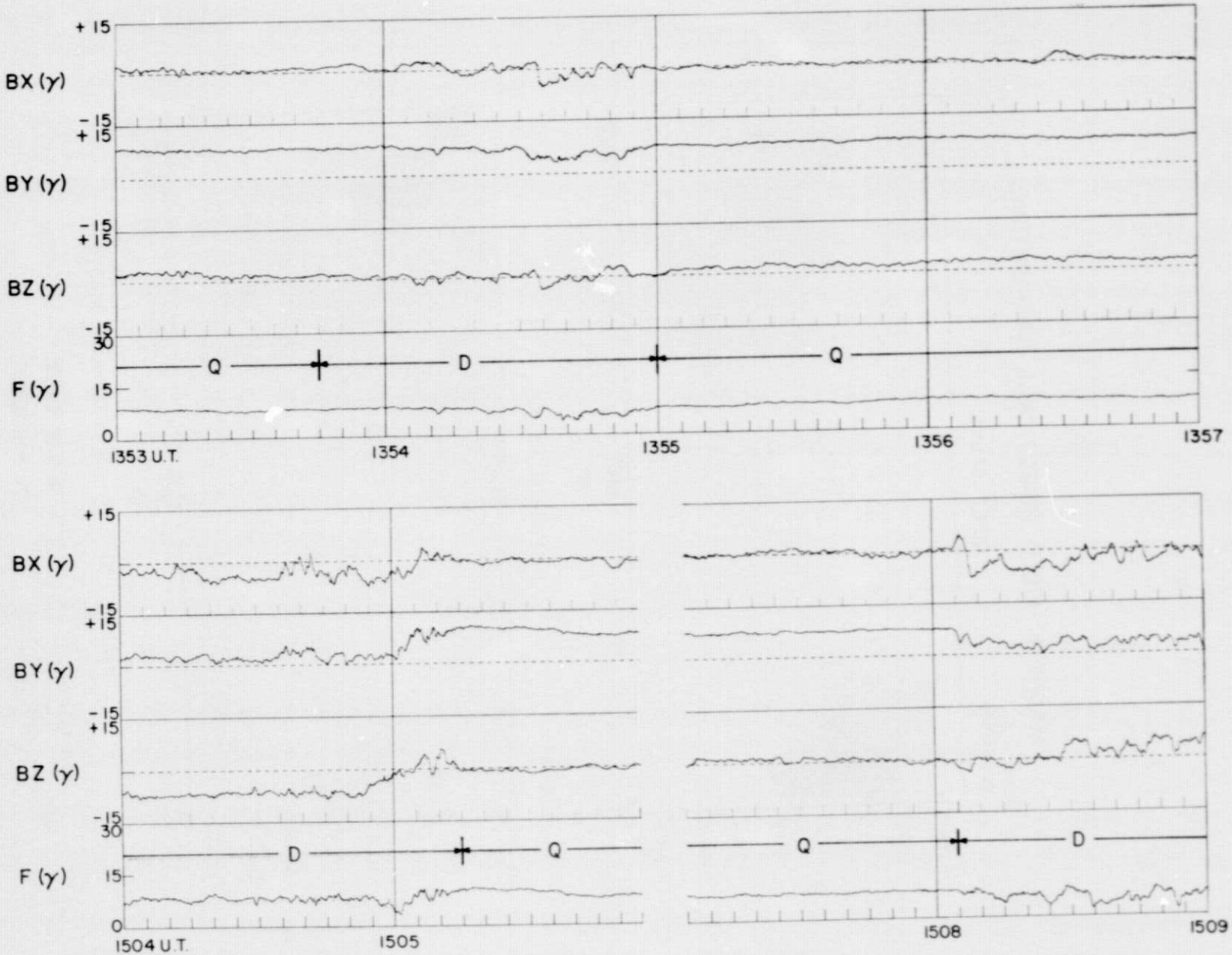

FEBRUARY 5, 1974

Figure 8

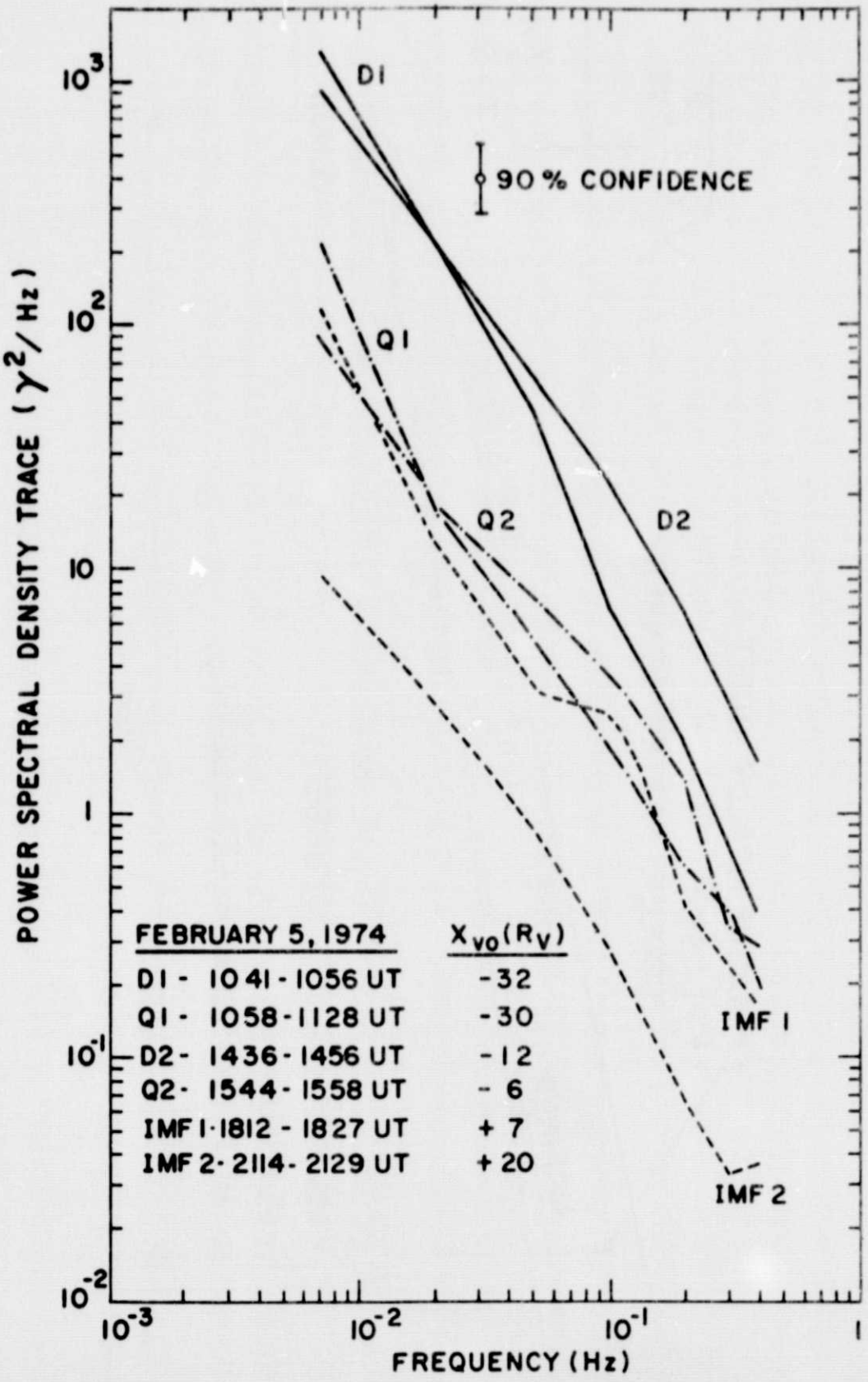
POWER SPECTRAL DENSITY TRACE (γ^2/Hz)
FREQUENCY (Hz)
10^3
10^2
10
1
10^{-1}
10^{-2}
10^{-3}
10^{-2}
10^{-1}
1
D1
90 % CONFIDENCE
Q1
Q2
D2
IMF 1
IMF 2
FEBRUARY 5, 1974
$X_{VO}(R_V)$
D1 - 1041 - 1056 UT -32
Q1 - 1058 - 1128 UT -30
D2 - 1436 - 1456 UT -12
Q2 - 1544 - 1558 UT - 6
IMF 1 - 1812 - 1827 UT + 7
IMF 2 - 2114 - 2129 UT + 20

Figure 9

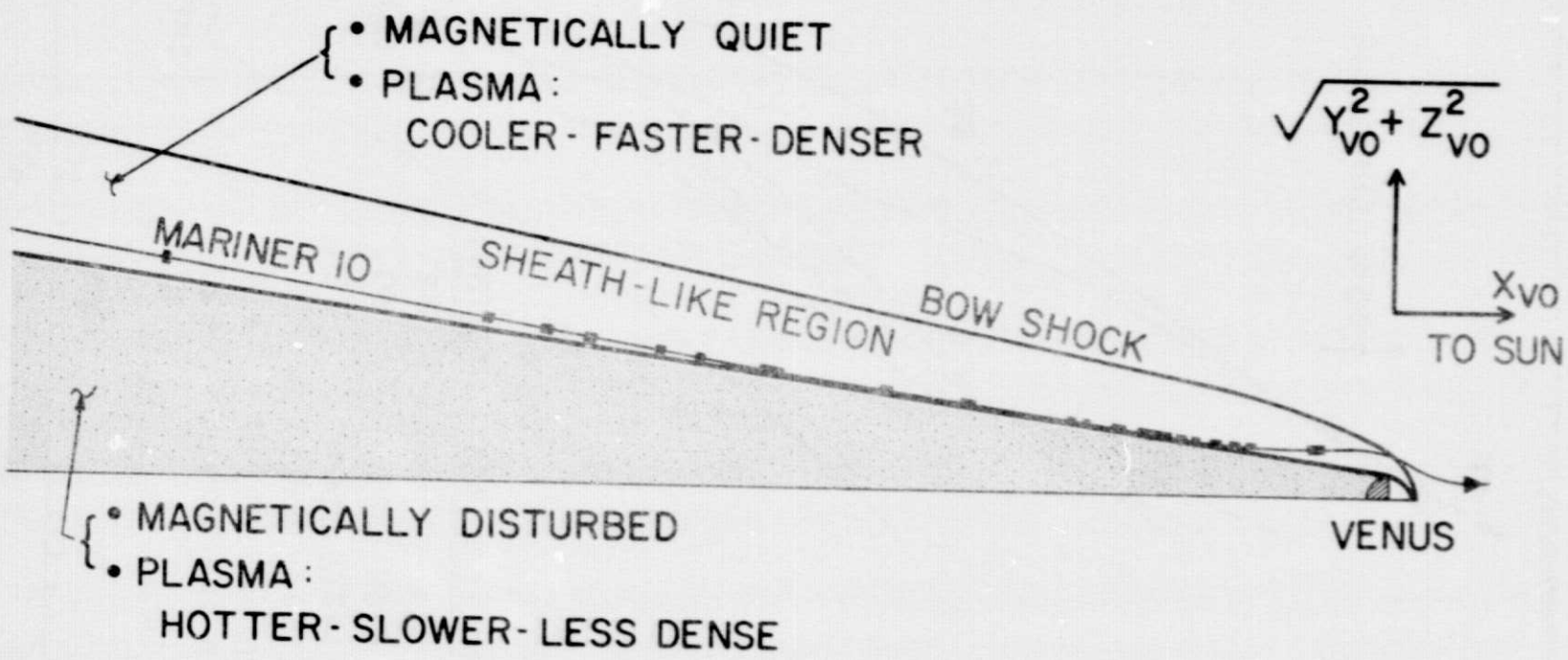
• MAGNETICALLY QUIET
• PLASMA:
COOLER - FASTER - DENSER
$\sqrt{Y_{VO}^2 + Z_{VO}^2}$
MARINER 10
SHEATH-LIKE REGION
BOW SHOCK
X_{VO}
TO SUN
• MAGNETICALLY DISTURBED
• PLASMA:
HOTTER - SLOWER - LESS DENSE
VENUS

Figure 10

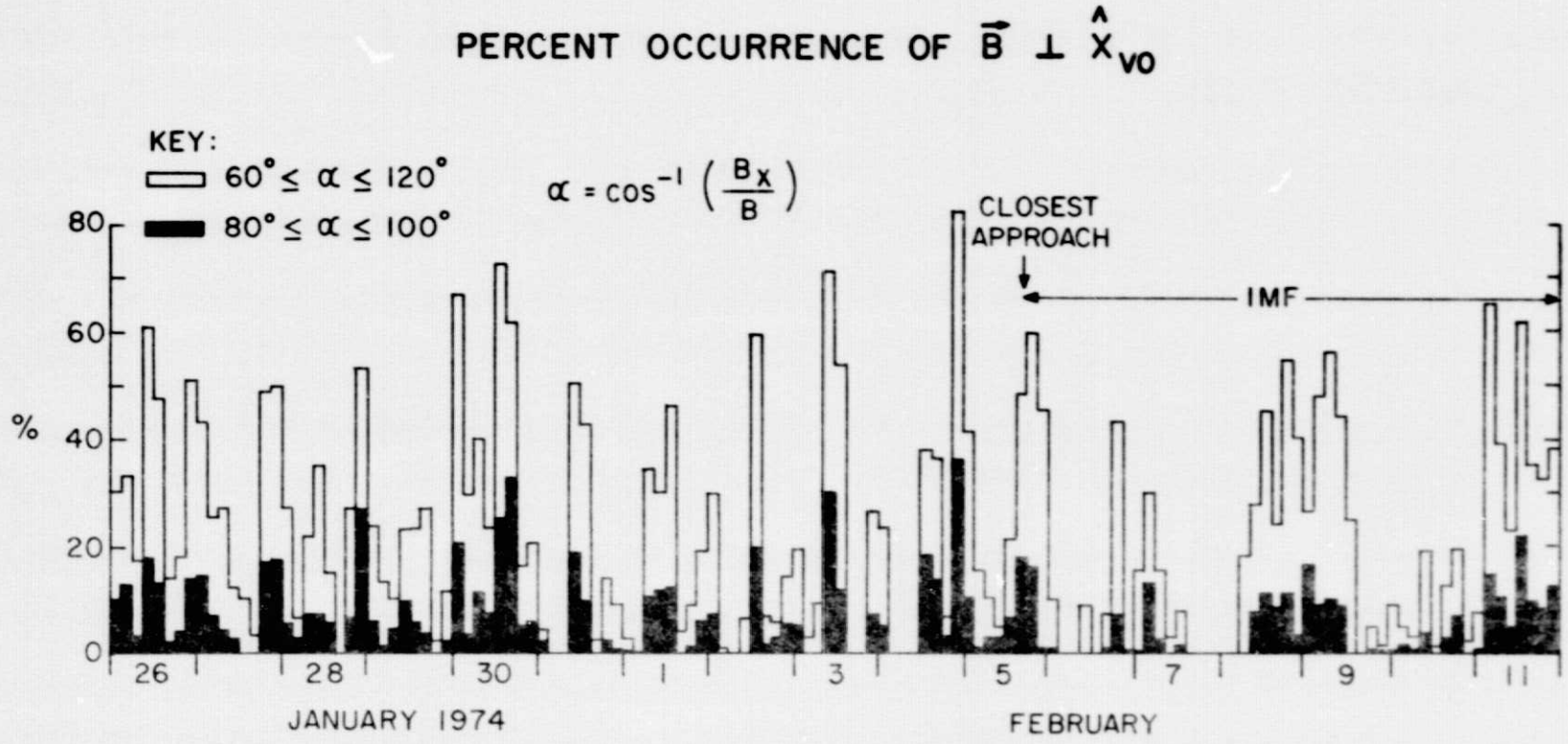
PERCENT OCCURRENCE OF $\vec{B} \perp \hat{X}_{VO}$
KEY:
$60° \leq \alpha \leq 120°$
$80° \leq \alpha \leq 100°$
$\alpha = \cos^{-1}\left(\frac{B_X}{B}\right)$
CLOSEST APPROACH
IMF
%
80
60
40
20
0
26
28
30
1
3
5
7
9
11
JANUARY 1974
FEBRUARY

Figure 11